JACS
JOURNAL OF THE AMERICAN CHEMICAL SOCIETY

COMMUNICATION

pubs.acs.org/JACS

Breaking Symmetry toward Nonspherical Janus Particles Based on Polyhedral Oligomeric Silsesquioxanes: Molecular Design, "Click" Synthesis, and Hierarchical Structure

Yiwen Li,[†] Wen-Bin Zhang,*[,†] I-Fan Hsieh,[†] Guoliang Zhang,[†] Yan Cao,[†] Xiaopeng Li,[‡] Chrys Wesdemiotis,[†,‡] Bernard Lotz,[§] Huiming Xiong,*[,∥] and Stephen Z. D. Cheng*[,†]

[†]College of Polymer Science and Polymer Engineering, Department of Polymer Science, and [‡]Department of Chemistry, The University of Akron, Akron, Ohio 44325, United States

[§]Institut Charles Sadron (CNRS-Université de Strasbourg), 23, Rue du Loess, F-67034 Strasbourg, France

[∥]Department of Polymer Science and Engineering, School of Chemistry and Chemical Engineering, Shanghai Jiao Tong University, Shanghai, 200240, China

Supporting Information

ABSTRACT: The design, synthesis, and self-assembly of a series of precisely defined, nonspherical, polyhedral oligomeric silsesquioxane (POSS)-based molecular Janus particles are reported. The synthesis aims to fulfill the "click" philosophy by using thiol−ene chemistry to efficiently install versatile functionalities on one of the POSS cages. In such a way, both the geometrical and chemical symmetries were broken to create the Janus feature. These particles self-organize into hierarchically ordered supramolecular structures in the bulk. For example, the Janus particle with isobutyl groups on one POSS and carboxylic groups on the other self-assembles into a bilayered structure with head-to-head, tail-to-tail arrangements of each particle, which further organize into a three-dimensional orthorhombic lattice. While the ordered structure in the layers was lost upon heating via a first-order transition, the bilayered structure persisted throughout. This study provides a model system of well-defined molecular Janus particles for the general understanding of their self-assembly and hierarchical structure formation in the condensed state.

In analogy to the double-faced Roman god Janus, De Gennes formally introduced in his Nobel lecture the concept of "Janus grains" to describe grains with two distinct sides.[1] The essential idea is that a three-dimensionally dissymmetrical distribution of certain physical/chemical features, such as size, shape, bulk composition, and surface chemistry, shall lead to the formation of specific hierarchical structures with novel properties.[2] It has since thrived into a dynamic research area and the "Janus" term has been extended to describe the "dissymmetrical entities" in general,[3] including macromolecules, supramolecular assemblies, nanoparticles, and colloidal particles. In synthesis, it requires the break of symmetry in the first place to create the "Janus" feature. So far, the synthesis of Janus particles based on inorganic nanoparticles and colloidal particles has been achieved by a number of methods, such as partial contact with reactive media,[4] directed fluxes and fields,[5] spontaneous assembly,[6] and controlled surface nucleation,[7] with a plethora of variations in sizes, shapes, and chemical compositions. Yet it remains a challenge to synthesize readily scalable, well-defined Janus particles with molecular precision and high uniformity, which limits the synthetic versatility and the formation of 3D long-range ordered structures. In this respect, molecular Janus entities, such as amphiphilic dendritic macromolecules,[8] unimolecular micelles of block copolymers,[9] and polymer brushes,[10] provide an intriguing alternative. Owing to their decreased sizes of typically only a few nanometers and the precisely defined molecular structures, they exhibit diverse self-assembled morphologies in the bulk,[8a] at the interface,[8c] or in solution.[8b,d−f] An extraordinary example was demonstrated by Percec et al. in the development of amphiphilic "Janus dendrimers" that spontaneously form various morphologies in water.[8b] Nevertheless, unlike "hard" colloidal Janus particles, the molecular Janus entities reported so far are often not "volume-persistent" or "shape-persistent" due to the flexibility of conformations. In addition, it requires multiple-step synthesis involving delicate control over reaction conditions and nontrivial purifications. Thus, it is of great interest to develop molecular Janus entities that are readily available, only a few nanometers in size, 3D volume- and shape-persistent, and that can self-assemble into hierarchical structures of potential technological importance.

Here, we report our first effort toward this goal by the design and synthesis of polyhedral oligomeric silsesquioxane (POSS)-based molecular Janus particles and the elucidation of their self-assembled, hierarchical structures in the bulk. POSS, perhaps the smallest silicon nanoparticles with cage diameter around 1.0 nm, are versatile nanobuilding blocks that are conformationally rigid and shape-persistent with diverse periphery functionalities.[11] As a route to "Janus silsesquioxanes", selective/nonselective functionalization of the POSS cage has been proposed in order to break the high symmetry of the cage and create the Janus feature.[12] Though fundamentally interesting, nontrivial optimization is required to promote both the selectivity of the process and the purity of the final product. Instead, the current molecular design chose to connect two POSS of distinct surface chemistry to create the Janus nature (Scheme 1). By monofunctionalization, the symmetry of POSS cage is reduced from O_h to C_{3v}; by coupling of two POSSs, the overall molecular shape changes from spherical to dumbbell- or snowman-like. Despite the same "bulk" composition for both halves, the difference in surface chemistry comprises the major driving force for self-assembly. Facilitated by "click"

Received: March 30, 2011
Published: June 16, 2011

Scheme 1. General Synthetic Strategy for BPOSS-XPOSS Janus Particles[a]

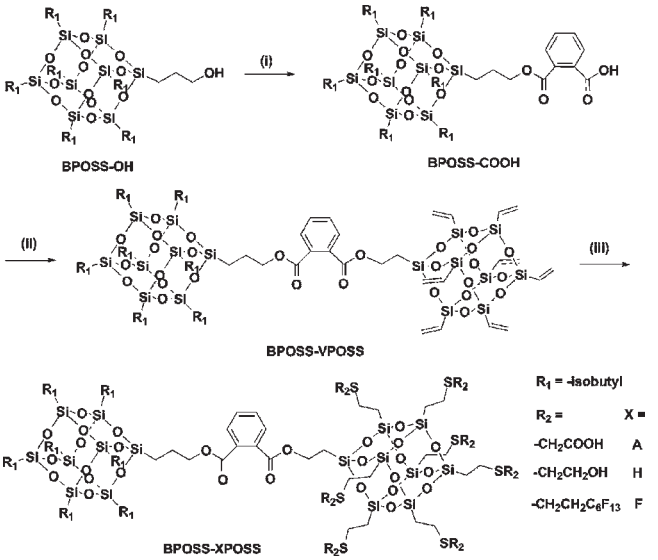

[a] (i) Phthalic anhydride, DMAP, triethylamine, THF, rt, 90%; (ii) PSS-(3-hydroxyethyl)-heptavinyl substituted (VPOSS-OH), DMAP, DIPC, dry CH_2Cl_2, 0 °C, 93%; (iii) R_2SH, DMPA, THF, rt, 15 min, 77−83%.

chemistry, the simultaneous control over size, shape, and surface chemistry provides a series of precisely defined, model molecular Janus particles for a systematic study of their self-assembly and properties.

The synthetic strategy is outlined in Scheme 1, where we strive to fulfill the "click" philosophy by modular construction of diverse materials from a set of simple building blocks and efficient chemical reactions. In literature, various well-defined functional POSS cages with distinct periphery functionalities, such as carboxylic acids, hydroxyls,[13] perfluorinated chains,[14] and bioactive moieties,[15] have been reported. The synthetic methods include metal-catalyzed cross-coupling reactions,[16] olefin metathesis,[17] Cu(I)-catalyzed Huisgen [3 + 2] cycloadditions,[15a] and thiol−ene "click" chemistry.[13,14,15b] Here, the common precursor BPOSS-VPOSS was prepared from commercially available BPOSS-OH in two steps by alcoholysis of phthalic anhydride and esterification with VPOSS-OH in excellent yields (>90%). The functionalization of BPOSS-VPOSS using thiol−ene chemistry proceeds in high efficiency under mild conditions (∼100% conversion), as evidenced by the complete disappearance of signals of vinyl protons in ^{1}H NMR spectra of the crude product, which is remarkable in view of multiple reactive sites and short reaction time involved. Specifically, carboxylic acid groups, hydroxyl groups, and short perfluorinated chains have been successfully installed on VPOSS to generate APOSS, HPOSS, and FPOSS, respectively, in ∼80% yield after workup and purification. These nonspherical molecular Janus particles (BPOSS-XPOSS) were thoroughly characterized by ^{1}H NMR, ^{13}C NMR, FT-IR, and MALDI-TOF mass spectrometry to confirm their identity (see Supporting Information). The most convincing evidence was provided by the MALDI-TOF mass spectra (Figure 1) where only one strong peak matching the proposed structures of the targeted molecules was observed. For example, the observed peak at m/z 2321.44 of $[BPOSS\text{-}APOSS\cdot Na]^+$ agrees well with the calculated monoisotopic molecular mass (2321.21 Da) (Figures 1 and S3a). Physically, all the BPOSS-XPOSS are powders readily soluble in common organic solvents such as THF and $CHCl_3$. The solubilities of BPOSS-APOSS and

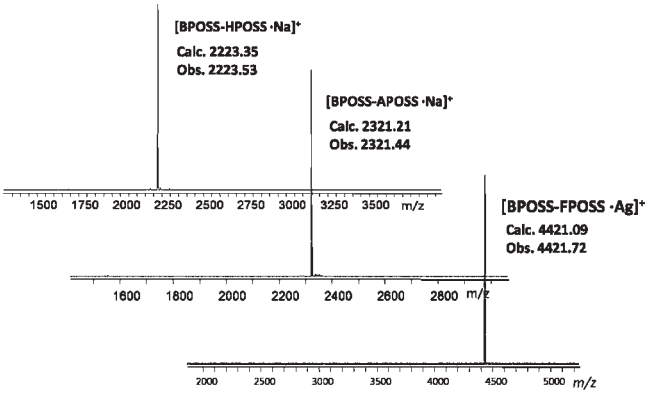

Figure 1. MALDI-TOF mass spectra of BPOSS-XPOSS.

BPOSS-HPOSS in methanol and ethanol are much increased compared to BPOSS-VPOSS. Under basic conditions, BPOSS-APOSS can dissolve in water. Their dual solubility reflects the amphilicity and the Janus feature. Notably, the reaction can be readily scaled up, facilitating preparation of gram quantities of samples and the study of their physics. The exemplary elucidation of the self-assembled structure of BPOSS-APOSS in the bulk is shown below.

The phase behavior of BPOSS-APOSS was first examined by differential scanning calorimetry (DSC) at a rate of 10 °C/min, as shown in Figure 2a. The first cooling thermal diagram exhibits an exothermic transition peaked at 141 °C with a latent heat of 18.6 kJ/mol. The subsequent heating shows an endothermic transition peaked at 182 °C with an essentially identical latent heat (18.8 kJ/mol). It is therefore a first-order transition in the condensed state associated with the ordered structure formation under supercooling. The temperature-dependent simultaneous SAXS-WAXD experiments on a BPOSS-APOSS sample were then performed (Figures S4 and S5). At room temperature, the patterns suggest the formation of a hierarchically ordered structure in the bulk (Figure 2c,d) and the diffraction patterns cover the length scale from a few angstroms to several nanometers. In the SAXS pattern (Figure 2c), two distinct peaks appear with a q ratio of 1:2, indicating a layered supramolecular structure with a spacing of 4.62 nm. This is close to twice the length of the long axis of BPOSS-APOSS (4.78 nm), suggesting a bilayered structure. The halo near q_1 peak may be attributed to the disordered aggregates and, thus, a correlation hole scattering.[18] In the WAXD pattern (Figure 2d), several sharp diffraction peaks represent the existence of an ordered structure on the angstrom scale, which are largely attributed to the ordered packing within the bilayers with segmental order of the molecules. Except for the first diffraction peak that can be assigned as the (004) diffraction of the layered structure in Figure 2d (d-spacing of 1.16 nm), the rest of the diffractions should be attributed to the 3D ordered structure within the bilayers. Note that, in the wide angle region, there are also two correlation hole scatterings (one is located at ∼6°, and the other at ∼14°). Although the diffractions at the wide angle region, except the (004) diffraction, disappear above 182 °C upon heating and reappear at 140 °C during cooling (Figure S5), the diffractions associated with the bilayer structure at the low angle region persist throughout (Figure S4). Nevertheless, there is a discontinuous change in the spacing of this bilayered structure from 4.80 to 4.70 nm at 140 °C during cooling (Figure 2b). This is another manifestation of a thermodynamic first-order transition. From the structural point of view, this transition is associated with the ordering of the supramolecular bilayered liquid crystal phase into the crystalline phase.

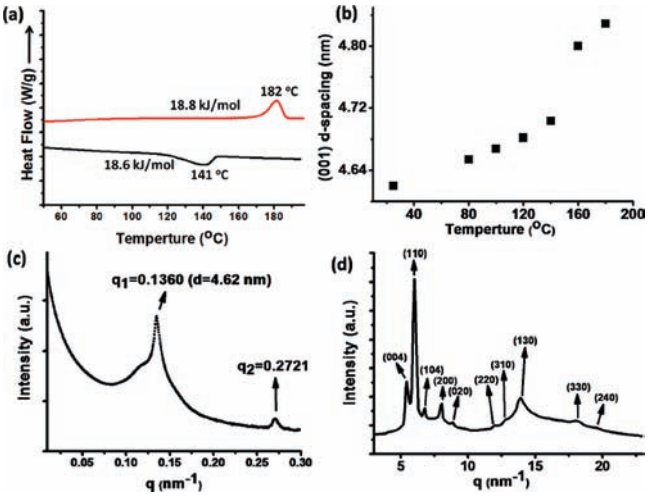

Figure 2. DSC heating and subsequent cooling diagrams (a), the change of layer spacing with temperature during the cooling process (b), SAXS pattern (c), and WAXD pattern (d) of thermally annealed BPOSS-APOSS.

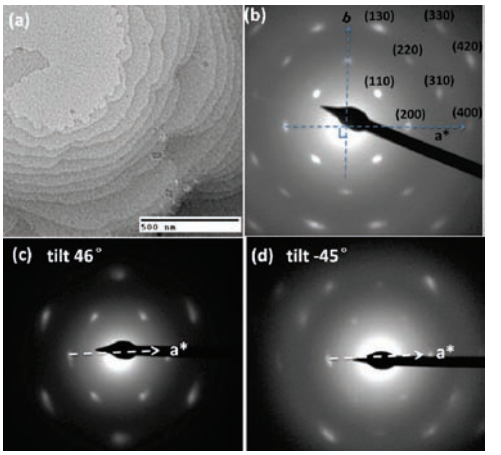

Figure 3. (a) TEM bright field image of the thermal annealed BPOSS-APOSS film; (b) SAED pattern of the [001] zone without tilting obtained from the sample in (a). SAED patterns of (c) and (d) were obtained by tilting the sample by 46° and −45° from the [001] zone around a^*-axis, respectively.

To determine the detailed lattice parameters and symmetry group of the ordered structure of BPOSS-APOSS, selected area electron diffraction (SAED) was performed in transmission electron microscopy (TEM). The detailed procedure for TEM sample preparation is included in the Supporting Information. Figure 3a shows a typical TEM bright field image of the BPOSS-APOSS film, which reveals stacked lamellar morphology with a flat-on arrangement. The presence of granular structures is due probably to the fast solvent removal during the film preparation. With increasing the annealing time at 140 °C, substantial decrease of the granular structures in the lamellar morphology was observed. We speculate that the correlation hole scattering observed in Figure 2c may be associated with this granular structure. In Figure 3b, the SAED pattern was obtained along the [001] zone and the extinct spots on the SAED pattern suggest a 2D rectangular symmetry (*p2gg*). The dimensions of the unit cell can be determined as a = 1.53 nm, b = 1.43 nm, and γ = 90°. The determination of c-axis dimension and α and β angles rely on the tilted ED experiments. Panels c and d of Figure 3 show two ED patterns at tilting angles of 46° and −45° around the a^*-axis, respectively, giving the c-axis dimension as 4.62 nm, which is identical to the layer spacing determined by SAXS (Figure 2b). Both α and β are determined to be 90°. It is thus an orthorhombic unit cell with a symmetry group of $Pna2_1$. In addition, the calculated crystallographic density is 1.51 g/cm^3 based on four BPOSS-APOSS molecules within each unit cell, which matches well with the experimental value of 1.49 g/cm^3. The lower experimental value is due to the fact that the bulk sample is not composed of 100% crystalline structures (see Figure 2c,d for the correlation hole scatterings). The thickness of each lamella shown in Figure 3a can be measured using atomic force microscopy (AFM). Indeed, the multilayer lamellar structure was also observed in the phase mode of AFM (Figure S6a). The vertical height scanning profiles (Figure S6b,d) reveal that the thickness of each layer is between 4.6 and 4.9 nm. This is in a good agreement with the SAXS and SAED results, suggesting that each lamella only has the dimension of one single unit cell along the c-axis in a flat-on arrangement.

The most probable molecular packing of BPOSS-APOSS in the orthorhombic unit cell was illustrated via computer simulation by the Accelrys Cerius^2 package using the universal force field. The results are shown in Figure 4. The atomic packing can be better represented by the spacing filling model as shown in Figure S8. Along the c-axis, the bilayered structure is unambiguous with a head-to-head, tail-to-tail packing orientation of BPOSS-APOSS parallel to the layer normal. The *ab*-crystalline planes are thus alternatively arranged with BPOSS or APOSS bilayers. In addition, the geometrical symmetry breaking induced by the covalent linkage actually leads to a small tilt of one set of POSS edges away from the c-axis toward the b-axis and the other set of POSS edges titling less toward the a-axis. To achieve the minimum free energy of crystal packing in our simulation, the tilt angle is alternatively positive (clockwise) and negative (anticlockwise) with respect to the c-axis along the layer normal (Figure 4a). This causes the slight difference between the a and b dimensions (Figure 4b). The computer-simulated ED patterns along the [001], [04−1] and [041] zones (Figures 4d and S7) are in quantitative agreement with the experimental ones in terms of both position and intensity (Figure 3b−d), which indicates that the proposed overall symmetry and molecular packing are correct reflections of the reality.

The next question is the rationale for the formation of such a bilayered structure and its implications on the self-assembly of Janus particles in the bulk. The covalent linkage between two distinct POSS is responsible for the symmetry breaking in shape, while the dissymmetry in surface chemistry on POSS is the driving force for the self-assembly due to the specific interactions such as hydrogen bonding (Figure S9). It should be noted that, if surface functional groups on two POSSs are not completely immiscible such as BPOSS-VPOSS, the hierarchical bilayer structure was not observed (Figure S10). Only when both POSSs are commensurate in shape and volume but immiscible with respect to surface functionalities, their rigid, large building blocks will lead to a nanoscale segregation of POSS to form bilayered structure. In addition, the functional groups within each layer can further self-organize into crystalline order at the angstrom level. The structure is thus hierarchical by design. If the volumes are incommensurate as in the case of "snowman-like" Janus particles, the formation of ordered structures would require more delicate balance in molecular design among the volume ratios, chemical interactions, and packing considerations. The relevant study is currently ongoing in our group using these model molecular Janus particles.

In summary, a series of precisely defined "dumbbell-like" or "snowman-like" POSS-based molecular Janus particles has been synthesized by covalently linking together two POSS cages with

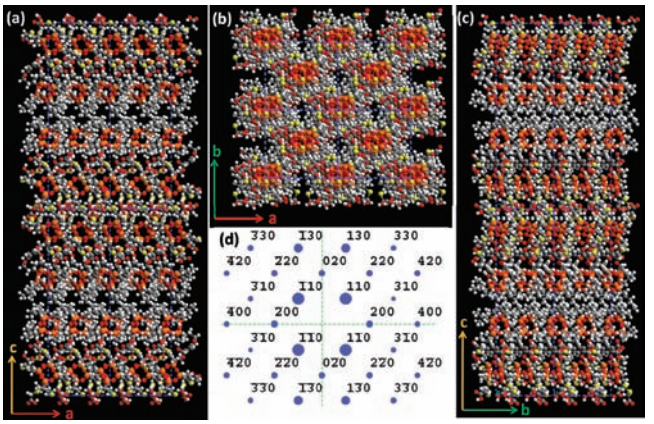

Figure 4. Molecular packing of BPOSS-APOSS in the crystal lattice on different planes. (a) *ac*-plane when projected from *b*-axis direction; (b) *ab*-plane when projected from *c*-axis direction; (c) *bc*-plane when projected from *a*-axis direction; (d) computer-simulated ED pattern along the [001] zone.

distinct surface chemistry. Enabled by thiol−ene "click" chemistry, the synthetic strategy provides easy access to a class of model Janus particles with readily tunable molecular shape and surface chemistry for versatile self-assembly manipulation. To the best of our knowledge, BPOSS-APOSS may be the first reported Janus particle that can self-assemble into hierarchical structures in the bulk. It was found to exhibit a bilayered lamellar morphology in the bulk with an orthorhombic unit cell (a = 1.53 nm, b = 1.43 nm, c = 4.62 nm) and a symmetry group of $Pna2_1$. While the crystalline order can be lost upon heating, the bilayered structure persists throughout. The driving force of the hierarchical structure formation can be attributed to the free energy minimization guided by the symmetry breaking in both geometry (overall molecular shape) and chemistry (amphiphilic interactions). The study introduces POSS-based molecular Janus particles as a new class of amphiphiles and an intermediate between colloidal Janus particles and molecular Janus entities. It has further implications on the understanding of the self-assembly behavior of Janus particles in general.

■ ASSOCIATED CONTENT

Supporting Information. Synthesis, characterization, and simulation data. This material is available free of charge via the Internet at http://pubs.acs.org.

■ AUTHOR INFORMATION

Corresponding Authors
wz8@uakron.edu; hmxiong@stju.edu.cn; scheng@uakron.edu

■ ACKNOWLEDGMENT

This work was supported by the National Science Foundation (DMR-0906898).

■ REFERENCES

(1) De Gennes, P.-G. *Angew. Chem., Int. Ed.* **1992**, *31*, 842–845.
(2) (a) Jiang, S.; Chen, Q.; Tripathy, M.; Luijten, E.; Schweizer, K. S.; Granick, S. *Adv. Mater.* **2010**, *22*, 1060–1071. (b) Lee, K. J.; Yoon, J.; Lahann, J. *Curr. Opin. Colloid Interface Sci.* **2010**, *16*, 195–202. (c) Walther, A.; Müller, A. H. E. *Soft Matter* **2008**, *4*, 663–668. (d) Wurm, F.; Kilbinger, A. F. M. *Angew. Chem., Int. Ed.* **2009**, *48*, 8412–8421. (e) Granick, S.; Jiang, S.; Chen, Q. *Phys. Today* **2009**, *62*, 68–69.
(3) (a) Kretzschmar, I.; Song, J. H. K. *Curr. Opin. Colloid Interface Sci.* **2011**, *16*, 84–95. (b) Perro, A.; Reculusa, S.; Ravaine, S.; Bourgeat-Lami, E.; Duguet, E. *J. Mater. Chem.* **2005**, *15*, 3745–3760. (c) Reculusa, S.; Poncet-Legrand, C.; Perro, A.; Duguet, E.; Bourgeat-Lami, E.; Mingotaud, C.; Ravaine, S. *Chem. mater.* **2005**, *17*, 3338–3344. (d) Duguet, E.; Désert, A.; Perro, A.; Ravaine, S. *Chem. Soc. Rev.* **2011**, *40*, 941–960. (e) Roh, K.-H.; Martin, D. C.; Lahann, J. *Nat. Mater.* **2005**, *4*, 759–763. (f) Glotzer, S. C.; Solomon, M. J. *Nat. Mater.* **2007**, *6*, 557–562. (g) Palmer, L. C.; Velichko, Y. S.; De La Cruz, M. O.; Stupp, S. I. *Philos. Trans. R. Soc., A* **2007**, *365*, 1417–1433.
(4) Dendukuri, D.; Pregibon, D. C.; Collins, J.; Hatton, T. A.; Doyle, P. S. *Nat. Mater.* **2006**, *5*, 365–369.
(5) (a) Nie, Z.; Li, W.; Seo, M.; Xu, S.; Kumacheva, E. *J. Am. Chem. Soc.* **2006**, *128*, 9408–9412. (b) Nisisako, T.; Torii, T.; Takahashi, T.; Takizawa, Y. *Adv. Mater.* **2006**, *18*, 1152–1156. (c) Shepherd, R. F.; Conrad, J. C.; Rhodes, S. K.; Link, D. R.; Marquez, M.; Weitz, D. A.; Lewis, J. A. *Langmuir* **2006**, *22*, 8618–8622.
(6) (a) Walther, A.; André, X.; Drechsler, M.; Abetz, V.; Müller, A. H. E. *J. Am. Chem. Soc.* **2007**, *129*, 6187–6198. (b) Liu, Y.; Abetz, V.; Müller, A. H. E. *Macromolecules* **2003**, *36*, 7894–7898.
(7) (a) Yang, J.; Elim, H. I.; Zhang, Q.; Lee, J. Y.; Ji, W. *J. Am. Chem. Soc.* **2006**, *128*, 11921–11926. (b) Gu, H.; Zheng, R.; Zhang, X.; Xu, B. *J. Am. Chem. Soc.* **2004**, *126*, 5664–5665.
(8) (a) Percec, V.; Imam, M. R.; Bera, T. K.; Balagurusamy, V. S. K.; Peterca, M.; Heiney, P. A. *Angew. Chem., Int. Ed.* **2005**, *44*, 4739–4745. (b) Percec, V.; et al. *Science* **2010**, *328*, 1009–1014. (c) Yang, M.; Wang, W.; Lieberwirth, I.; Wegner, G. *J. Am. Chem. Soc.* **2009**, *131*, 6283–6292. (d) Yang, M.; Wang, W.; Yuan, F.; Zhang, X.; Li, J.; Liang, F.; He, B.; Minch, B.; Wegner, G. *J. Am. Chem. Soc.* **2005**, *127*, 15107–15111. (e) Yuan, F.; Zhang, X.; Yang, M.; Wang, W.; Minch, B.; Lieser, G.; Wegner, G. *Soft Matter* **2007**, *3*, 1372–1376. (f) Yang, M.; Zhang, Z.; Yuan, F.; Wang, W.; Hess, S.; Lienkamp, K.; Lieberwirth, I.; Wegner, G. *Chem.—Eur. J.* **2008**, *14*, 3330–3337.
(9) Cheng, L.; Hou, G.; Miao, J.; Chen, D.; Jiang, M.; Zhu, L. *Macromolecules* **2008**, *41*, 8159–8166.
(10) (a) Cheng, G.; Böker, A.; Zhang, M.; Krausch, G.; Müller, A. H. E. *Macromolecules* **2001**, *34*, 6883–6888. (b) Zhang, M.; Müller, A. H. E. *J. Polym. Sci., Part A: Polym. Chem.* **2005**, *43*, 3461–3481.
(11) (a) Wang, X.; Ervithayasuporn, V.; Zhang, Y.; Kawakami, Y. *Chem. Commun.* **2011**, *47*, 1282–1284. (b) Roll, M. F.; Asuncion, M. Z.; Kampf, J.; Laine, R. M. *ACS Nano* **2008**, *2*, 320–326. (c) Cui, L.; Collet, J. P.; Xu, G.; Zhu, L. *Chem. Mater.* **2006**, *18*, 3503–3512. (d) Miao, J.; Zhu, L. *J. Phys. Chem. B.* **2010**, *114*, 1879–1887. (e) Pielichowski, K.; Njuguna, J.; Janowski, B.; Pielichowski, J. *Adv. Polym. Sci.* **2006**, *201*, 225–296. (f) Cordes, D. B.; Lickiss, P. D.; Rataboul, F. *Chem. Rev.* **2010**, *110*, 2081–2173.
(12) (a) Laine, R. M.; Roll, M.; Asuncion, M.; Sulaiman, S.; Popova, V.; Bartz, D.; Krug, D. J.; Mutin, P. H. *J. Sol-Gel Sci. Technol.* **2008**, *46*, 335–347. (b) Asuncion, M. Z.; Ronchi, M.; Abu-Seir, H.; Laine, R. M. *C. R. Chim.* **2010**, *13*, 270–281. (c) Deng, J.; Polidan, J. T.; Hottle, J. R.; Farmer-Creely, C. E.; Viers, B. D.; Esker, A. R. *J. Am. Chem. Soc.* **2002**, *124*, 15194–15195.
(13) (a) Yu, X.; Zhong, S.; Li, X.; Tu, Y.; Yang, S.; Van Horn, R. M.; Ni, C.; Pochan, D. J.; Quirk, R. P.; Wesdemiotis, C.; Zhang, W.-B.; Cheng, S. Z. D. *J. Am. Chem. Soc.* **2010**, *132*, 16741–16744. (b) Zhang, W.-B.; Li, Y.; Li, X.; Dong, X.; Yu, X.; Wang, C.-L.; Wesdemiotis, C.; Quirk, R. P.; Cheng, S. Z. D. *Macromolecules* **2011**, *44*, 2589–2596.
(14) (a) Xu, J.; Li, X.; Cho, C. M.; Toh, C. L.; Shen, L.; Mya, K. Y.; Lu, X.; He, C. *J. Mater. Chem.* **2009**, *19*, 4740–4745. (b) Mabry, J. M.; Vij, A.; Iacono, S. T.; Viers, B. D. *Angew. Chem., Int. Ed.* **2008**, *47*, 4137–4140.
(15) (a) Fabritz, S.; Heyl, D.; Bagutski, V.; Empting, M.; Rikowski, E.; Frauendorf, H.; Balog, I.; Fessner, W.-D.; Schneider, J. J.; Avrutina, O.; Kolmar, H. *Org. Biomol. Chem.* **2010**, *8*, 2212–2218. (b) Gao, Y.; Eguchi, A.; Kakehi, K.; Lee, Y. C. *Org. Lett.* **2004**, *6*, 3457–3460.
(16) Roll, M. F.; Asuncion, M. Z.; Kampf, J.; Laine, R. M. *Acs Nano* **2008**, *2*, 320–326.
(17) Feher, F. J.; Soulivong, D.; Eklund, A. G.; Wyndham, K. D. *Chem. Commun.* **1997**, 1185–1186.
(18) Bates, F. S. *Macromolecules* **1985**, *18*, 525–528.